International Journal of Academic Research and Development
ISSN: 2455-4197
Impact Factor: RJIF 5.22
www.academicsjournal.com
Volume 3; Issue 1; January 2018; Page No. 267-276

Synthesis, spectral, electrochemical characterization and application of Co(II), Ni(II), Cu(II) and Zn(II) complexes of novel Schiff base ligands

P Chandra Menaga, V Rama
PG & Research, Department of Chemistry, Sarah Tucker College, Manonmaniam Sundaranar University, Tirunelveli, Tamil Nadu, India

Abstract
A new series of transition metal complexes of Co(II), Ni(II), Cu(II) and Zn(II) were synthesized from the Schiff base ligands: 4-(4-aminophenylsulfonyl)-N-(thiophene-2-ylmethylene)aniline (SB1) and 4-(4-aminophenyl sulfonyl)-N-(3,4-dimethoxybenzylidene) aniline (SB2). All the prepared compounds were characterized by elemental analysis, molar conductivity, magnetic susceptibility, IR, UV-visible spectroscopy, H^1 NMR and C^{13} NMR. From the physicochemical studies and spectral data, the ligands were found to be bidentate with the general composition $[M(L)_2Cl_2]$ [Where M= Co(II), Ni(II), Co(II) and Zn(II); L = Schiff base Ligand]. The lower conductivity data confirmed the non-electrolytic nature of the complexes. The corrosion inhibition characteristics of Schiff base ligands and their metal complexes on mild steel in 0.1 M HCl solution was studied by chemical method. The adsorption of inhibitors on mild steel surface obeyed Langmuir, Frumkin and Temkin adsorption isotherm. The calculated thermodynamic parameters for adsorption reveal a strong interaction between the inhibitors and the mild steel surface. The ligands and their metal complexes were screened for their antimicrobial and found to exhibit moderate to good activity.

Keywords: schiff bases, metal complexes, 4, 4'-sulfonyldianiline, 2-thiophenecarboxaldehyde, 3,4dimethoxybenzaldehyde

Introduction
Metal complexes had been receiving considerable attention for many years, due to their interesting characteristics in the field of material science and biological systems. Schiff bases which were characterized by the –N=CH– (imines) group was important in elucidating the mechanism of transamination and racemisation reactions in biological systems [1, 2] and have high affinity to chelate with the transition metal ions. Hence have attracting attention due to potential applications in areas viz. biology, catalysis, thermal, electrical, optical, magnetic etc [3, 4]. In recent years, there had been enhanced interest in the synthesis and characterization of transition metal complexes containing Schiff bases as ligands due to their importance of antimicrobial, antibacterial, antifungal, anti-inflammatory, antitumor and anti HIV activities [5, 6].

Metal-based drugs are a research area of increasing interest for inorganic, pharmaceutical and medicinal chemistry and the researcher had concentrated much attention as an approach to new drug development. The sulfa drug derivatives widely used in clinical medicine as pharmacological agents with a wide variety of biological actions [7, 8]. One of the sulfa drug, 4, 4-diaminodiphenylsulphone (Dapsone), had been used particularly in the treatment of leprosy and also it has good antibacterial activity. This antileprosy drug was a very potent chelating agent and its effective coordination to metal ion may have significance biological implication [9].

Several research papers have reported the synthesis and characterization of transition metal complexes derived from 4, 4'-Sulfonyldianiline [10-14]. A search through literature revealed that no work had been reported on the transition metal complexes of the Schiff base 4,4diaminodiphenylsulphone with 2-thiophenecarboxaldehyde and 3,4dimethoxybenzaldehyde**.** Herein we had reported the synthesis, characterization, electrochemical analysis, anticorrosion and antimicrobial studies of transition metal complexes containing Schiff base ligands 4-(4-aminophenylsulfonyl)-N-(thiophene-2-ylmethylene) aniline (SB1) and 4-(4-aminophenylsulfonyl)-N-(3,4-dimethoxy-benzylidene) aniline (SB2).

2. Material and Methods
2.1. Chemicals and Reagents
All the chemicals and solvents of Sigma Aldrich/ Merck were AR grade and used without any further purification. Melting points of all the synthesized compounds were determined in open glass capillaries and were uncorrected. Purity of the compounds was checked by TLC and the spots were observed in iodine vapor.

2.2. Instrumentation
Electronic spectra of the Co (II), Ni (II), Cu (II) and Zn (II),complexes were recorded on a Systronic double beam spectrometer in quartz cells in the range 200–800 nm using 10^{-3}M solution in DMF. Molar conductance was measured on the ELICO (CM-185) conductivity bridge using 10^{-3} M solution in dry DMF by dip-type conductivity cell fitted with a platinum electrode. Magnetic susceptibility measurements were measured on a Gouy balance using Hg $[Co(NCS)_4]$ as the calibrant at room temperature. IR spectra were recorded by making KBr pellets on Jasco Fourier transform IR spectrophotometer. ^1H and ^{13}C NMR spectra were recorded on a Bruker 300 MHz spectrometer in DMSO-d_6 solvent. The elemental analysis was done on a Perkin-Elmer Analyzer 2440. The electrochemical behavior of the compounds was

investigated using the cyclic voltammetric (CV) technique in DMSO solution containing 0.1 M tetra (n-butyl) ammoniumperchlorate as the supporting electrolyte at scan rate 50 mVs^{-1}. The investigated potential range was -1.0 to 1.0 V, and displayed two well-defined electrode couples. Materials used for the corrosion study was mild steel sheet of composition (wt %, Mn (0.6), P (0.36), C (0.15) Si (0.03) and Fe (98.86). The sheet was mechanically pressed cut into different coupons, each of dimension, 4 x 2 x 0.05 cm. Each coupon was degreased by washing with ethanol, cleaned with acetone and allowed to dry in the air before preservation in a desiccator. All the synthesized compounds were screened for their antimicrobial activity using disc diffusion method.

2.3. Synthesis of Schiff base ligand 4-(4-aminophenylsulfonyl)-N-(thiophene-2-yl-methylene) aniline (SB1)

4,4-diaminodiphenylsulfone(dapsone) (0.01mol) and 2-thiophene carboxaldehyde (0.01mol) in hot methanol (50 ml) were mixed and refluxed for 8 hours. The reaction was monitored by TLC. Then the reaction mixture was kept overnight at room temperature and the resulting mixture was poured in crushed ice whereby precipitate was obtained. It was filtered off, washed several times with water recrystallized from ethanol and finally dried in a vacuum desiccator over anhydrous calcium chloride at room temperature (Scheme 1).

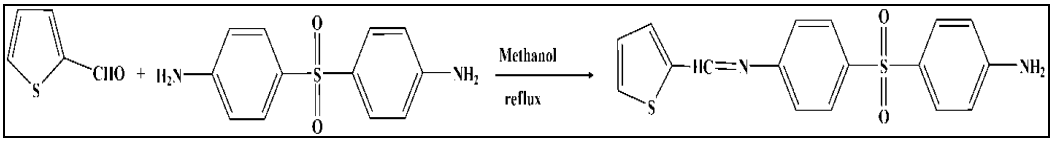

Scheme 1: Synthesis of ligand 4-(4-aminophenylsulfonyl)-N-(thiophene-2-ylmethylene) aniline (SB1)

2.4. Synthesis of Schiff base ligand 4-(4-aminophenylsulfonyl)-N-(3,4-dimethoxy-benzylidene) aniline (SB2)

4,4-diaminodiphenylsulfone (dapsone) (0.01mol) and 3, 4 dimethoxybenzaldehyde (0.01mol) in hot methanol (50 ml) were mixed and stirred for 4 hours. The reaction was Monitored by TLC and the reaction mixture was kept overnight at room temperature overnight. Yellow precipitate was obtained it was filtered off, washed several times with water, recrystallized from ethanol and finally dried in vacuum desiccators over anhydrous calcium chloride at room temperature (Scheme 2).

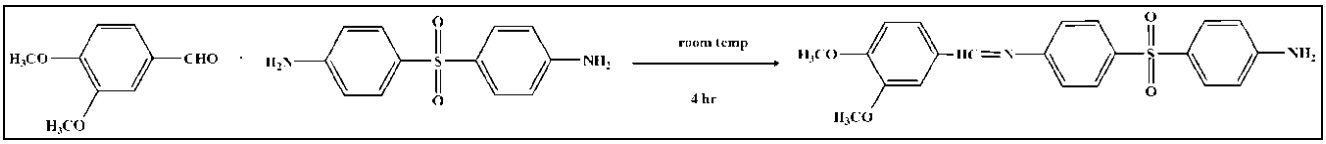

Scheme 2: Synthesis of ligand 4-(4-aminophenylsulfonyl)-N-(3, 4-dimethoxybenzylidene)aniline (SB2)

2.5. Synthesis of Schiff Base Metal Complexes

A hot ethanolic solution (20 ml) of ligand (0.02mol) and the corresponding metal salts (such as chlorides of Cu, Co, Ni and Zn (0.01mol)) were mixed together with constant stirring and refluxed for 3-4 hours at 70–80°C. On cooling, coloured complexes precipitated out. It was filtered metal complexes were collected, washed with distilled water then with ethanol and finally dried in a desiccator over anhydrous calcium chloride at room temperature.

2.6. Corrosion Study

2.6.1. Chemical Method

A blank solution of 1.0 M HCl and various concentration solutions of the inhibitors (SB1, SB2 and its metal complexes) were taken in a 100ml beaker and the steel specimens were suspended in the solution using glass hooks. Care was taken to ensure that the specimens were immersed completely in the solution and the specimens do not touch the walls of the beaker. After a period of three hours, the specimens were taken out, dried and weighed. From the initial and final weight of the specimen, weight loss was calculated. Inhibition efficiency was calculated from the weight loss of the specimen. From the average weight loss (mean of three replicate analyses) results, the corrosion rate of mild steel (ν), the inhibition efficiency (η_{WL}) of the inhibitor and the degree of surface coverage (θ) were calculated using equations 1 to 3 respectively,

$$\nu = W/St \quad (1)$$

$$\eta_{WL}(\%) = [(\nu_o - \nu)/\nu_o] \times 100 \quad (2)$$

$$\theta = [(\nu_o - \nu)/\nu_o] \quad (3)$$

Where W was the three-experimental average weight loss of the mild steel, S was the total surface area of the specimen, t was the immersion time and ν_o and ν were values of the corrosion rate without and with addition of the inhibitor, respectively.

2.6.2. Adsorption Isotherm and thermodynamic parameters

The mechanism of the interaction between inhibitor and the metal surface can be explained using adsorption Isotherms [15]. The degree of surface coverage (θ) was evaluated for different concentrations of the studied solutions from weight loss measurement with expression $\eta_{WL}\% = \theta \times 100$ which showed the relationship between surface coverage (θ) and inhibition efficiency (η_{WL} %). The adsorption of on mild steel surface obeys Langmuir, Frumkin and Temkin adsorption isothermal

equation [16],

$$\text{Langmuir: } C/\theta = (1/K) + C \quad (4)$$
$$\text{Frumkin: } \theta/(1-\theta)\exp(-2f\theta) = K_{ads}C_{ads} \quad (5)$$
$$\text{Temkin: } \exp(-2f\theta) = K_{ads}C_{ads} \quad (6)$$

θ was the surface coverage, K was the adsorption-desorption equilibrium constant, C was the concentration of inhibitor and f was the factor of energetic inhomogeneity. The free energy of adsorption $\Delta G^{o}_{ads,}$ enthalpy of adsorption (ΔH^{0}_{ads}) and entropy of adsorption (ΔS^{0}_{ads}) were calculated using the following equation as.

$$\Delta G^{\circ}_{ads} = -RT \ln(55.5\ K) \quad (7)$$
$$Ea = 2.303 \times RT \times \log(A/P) \quad (8)$$
$$\Delta H^{o}_{ads} = E_a - RT \quad (9)$$
$$\Delta S^{o}_{ads} = (\Delta H^{o}_{ads} - \Delta G^{o}_{ads})/T \quad (10)$$

Where 55.5 was the molar concentration of water, R was the universal gas constant and T was the temperature in K, Ea was the apparent activation energy. Results of corrosion rate and energy of activation also show similar trends as that for % I.E. The low and negative values of ΔG_{ads} indicate the spontaneous adsorption of the inhibitor on the surface of mild steel. The negative values of ΔG_{ads} were indicative of the strong interaction of the inhibitor molecules with the alloy surface. The values of heat of adsorption are higher than - 40 KJ mol^{-1} suggesting the chemical adsorption of the inhibitors[17]. It was an established fact that values of ΔG_{ads} around -20 KJ mol^{-1} or less indicates physisorption. The adsorption was attributed to the electrostatic attraction between the charged organic molecules and charged metal surface.

2.7. Antimicrobial Study

2.7.1 Antibacterial Activity

The *in-vitro* biological screening effects of the investigated compounds were tested against the bacteria *Escherichia coli, Pseudomonas aeruginosa, Klebsiella pneumonia, Proteus sps, Staphylococcus aureus, Enterococci sps and StarptoPneunomiae* by well diffusion method. The stock solutions were prepared by dissolving the compounds in DMSO All the blank discs were moistened with the solvent. For disc assays, the compounds containing disc (6 mm) with sample solution were placed on the surface of the nutrient plate previously spread with 0.1 ml of overnight culture of microorganisms. Then, the plates were incubated at 37°C for 48 hrs. During this period, the test solution was diffused and affected the growth of the microorganisms. Hence, the inhibition zones were developed on the plate around the disc. The antibacterial activity of common standard antibiotic chloramphenicol was also recorded using the same procedure as above at the same concentrations and solvent. The experiments were performed in triplicates.

2.6.2. Antifungal activity

The antifungal activities of the ligand and its metal complexes were tested against seven day cultures of *Aspergillus niger* and *candida albicans* using well diffusion method. The results show that the metal complexes were more active than free ligand and can be explained by Overtone's concept and Tweedy's chelation theory [18].

3. Result and Discussion

The complexes were found to be stable in air, non-hygroscopic, insoluble in water, ethanol and diethyl ether but completely soluble in DMF and DMSO. The physical properties and analytical data of the complexes were given in Table 1. Elemental analysis suggests that the complexes have 1: 2 (metal: ligand) molar ratio. The lower conductivity values of the complexes support the non-electrolytic nature of the metal complexes [19].

Table 1: Physical, analytical and molar conductance data of the Schiff base and its complexes

Mol. Formula	Mol. Weight	%Yield/ $Mp^{0}C$	Color/ Soluble In	Calculated (found)%				MolCon $.\Omega^{-1}cm^{2}mol^{-1}$
				C	N	S	Metal	
SB1 $C_{17}H_{14}N_2O_2S_2$	342.43	83.2/ 164	Brown/ Ethanol	59.63 (52.03)	8.18 (9.23)	18.73 (20.40)	-	-
$[Co(SB1)_2Cl_2]$ $C_{34}H_{28}N_4O_4S_4Cl_2Co$	814.7	70.5/ 138	Dark Brown/ DMSO,DMF	50.13 (52.74)	6.88 (5.89)	15.74 (17.54)	7.23 (7.10)	4.0
$[Ni(SB1)_2Cl_2]$ $C_{34}H_{28}N_4O_4S_4Cl_2Ni$	814.48	83.4/ 120	Light Brown/ DMSO,DMF	50.14 (49.23)	6.88 (5.40)	15.75 (14.50)	7.21 (7.9)	2.0
$[Cu(SB1)_2Cl_2]$ $C_{34}H_{28}N_4O_4S_4Cl_2Cu$	819.31	86.0/ 160	Pale yellow/ DMSO,DMF	49.84 (50.23)	6.84 (5.44)	15.65 (16.80)	7.76 (7.9)	3.0
$[Zn(SB1)_2Cl_2]$ $C_{34}H_{28}N_4O_4S_4Cl_2Zn$	821.15	81.5/ 202	Light Brown/ DMSO,DMF	49.73 (49.33)	6.82 (6.74)	15.62 (16.10)	7.76 (7.9)	8.9
SB2 $C_{21}H_{20}N_2O_4S$	396.46	92.5/ 104	Yellow/ Ethanol	63.62 (65.27)	7.07 (7.11)	8.09 (5.35)	-	-
$[Co(SB2)_2Cl_2]$ $C_{42}H_{40}N_4O_8S_2Cl_2Co$	922.76	94.5/ 160	Green/ DMSO,DMF	54.67 (53.55)	6.07 (6.81)	6.95 (6.01)	6.39 (6.20)	2.5
$[Ni(SB2)_2Cl_2]$ $C_{42}H_{40}N_4O_8S_2Cl_2Ni$	922.54	82.5/ 220	Orange / DMSO,DMF	54.68 (55.11)	6.07 (5.71)	6.95 (5.21)	6.36 (7.12)	3.2
$[Cu(SB2)_2\ Cl_2]$ $C_{42}H_{40}N_4O_8S_2Cl_2Cu$	927.37	87.4/ 130	Greenish yellow/ DMSO,DMF	54.4 (55.6)	6.04 (5.99)	6.91 (7.18)	6.85 (6.44)	5.0
$[Zn(SB2)_2\ Cl_2]$ $C_{42}H_{40}N_4O_8S_2Cl_2Zn$	929.21	80.0/ 196	Dark red/ DMSO,DMF	54.29 (54.6)	6.03 (5.78)	6.9 (6.79)	7.04 (7.54)	6.3

3.1. IR Spectra

The significant IR bands of the ligands and its metal complexes were observed for the establishment of the mode of the coordination of the ligands to the metal ion. The FTIR data of Schiff base ligands SB1, SB2 and their Co (II), Ni(II), and Cu(II) complexes were given in Table 2. There are some distinguished bands observed in the spectra of the complexes when compared to free ligand, which is helpful in detection of donation sites. In the spectrum of the Schiff base, the strong bands at 1613 and 1651 cm^{-1} were attributed to -CH=N groups [20]. On chelation, due to possible drift of lone pair electron density towards the metal ion, the azomethine -C=N band was expected to absorb at lower frequency in the complex. The bands at 3341and 3292 cm^{-1} were assigned to ν (NH_2) in the ligands and these bands were shifted significantly in the complexes which indicated the coordination of nitrogen of NH_2 group with metal. The bands at 1276, 1272 cm^{-1} and 1135, 1138 cm^{-1} were assigned to $\nu_{as}(SO_2)$ and $\nu_s(SO_2)$.These bands almost remained unchanged in the complexes which indicated the non-participation of SO_2 group in coordination [21]. The band at 719 cm^{-1} due to ν(C-S-C) of the thiophene ring remained unaltered in complexes indicating non-participation of the thiophene ring in coordination [22]. IR spectra of the complexes showed new peaks in the region at 590-544 cm^{-1} and 498-466 cm^{-1}region due to the formation of M-N bond and M-Cl bond respectively [23].

Table 2: IR Spectral data of the Schiff base and its complexes

Ligand/Compound No	ν max (cm^{-1})				
	ν(C=N)	ν(SO_2)	ν(NH_2)	ν(M-N)	ν(M-Cl)
SB1 $C_{17}H_{14}N_2O_2S_2$	1613	1276 1138	3341 3238	-	-
[Co(SB1)$_2$Cl$_2$] $C_{34}H_{28}N_4O_4S_4Cl_2Co$	1593	1286 1140	3383 3234	538	485
[Ni (SB1)$_2$Cl$_2$] $C_{34}H_{28}N_4O_4S_4Cl_2Ni$	1592	1284 1144	3371 3201	583	478
[Cu (SB1)$_2$Cl$_2$] $C_{34}H_{28}N_4O_4S_4Cl_2Cu$	1590	1279 1144	3368 3217	556	498
[Zn(SB1)$_2$Cl$_2$] $C_{34}H_{28}N_4O_4S_4Cl_2Zn$	1591	1280 1142	3370 3216	576	482
SB2 $C_{21}H_{20}N_2O_4S$	1651	1272 1135	3292 3053	-	-
[Co(SB2)$_2$Cl$_2$] $C_{42}H_{40}N_4O_8S_2Cl_2Co$	1580	1291 1151	3271 3052	544	466
[Ni(SB2)$_2$Cl$_2$] $C_{42}H_{40}N_4O_8S_2Cl_2Ni$	1548	1283 1147	3289 3050	590	488
[Cu(SB2)$_2$ Cl$_2$] $C_{42}H_{40}N_4O_8S_2Cl_2Cu$	1578	1285 1148	3271 3053	588	467
[Zn(SB2)$_2$ Cl$_2$] $C_{42}H_{40}N_4O_8S_2Cl_2Zn$	1566	1284 1149	3224 3051	582	477

3.2. Electronic spectra and magnetic moments

The electronic absorption spectra of the Schiff base metal complexes in solid state were recorded at room temperature and the band positions of the absorption maxima, band assignments, ligand field parameters, and magnetic moment values are listed in Table 3.

The UV/visible spectra for the Co(II) complex of ligands SB1 and SB2 showed three bands in the visible region at 436, 433, 737 nm and 431,439, 727 nm which were assigned to $^4T_{1g}$ (F) → $^4T_{2g}$ (F), $^4T_{1g}$(F) →$^4A_{2g}$(F) and $^4T_{1g}$(F) →$^4T_{1g}$(P) transitions respectively, which assume an octahedral geometry for Co(II) complex[24]. The electronic spectra of the Ni(II) complex of the Schiff base ligands SB1and SB2 showed three bands in the visible region at 422, 439, 763 and 415,433,765 nm which could assigned to $^3A_{2g}$(F) →$^3T_{2g}$(F),$^3A_{2g}$(F) →$^3T_{1g}$(F) and $^3A_{2g}$(F) →$^3T_{1g}$(P). This indicate octahedral geometry of the Ni(II) complex[25]. The electronic spectra of the Cu(II) complex of the Schiff base ligands SB1 and SB2 displayed one band in the visible region at 742 and 740 nm which could be assigned to ^2E_g→ $^2T_{2g}$. This indicate the octahedral geometry of the Cu(II) complex. Zn(II) complexes showed two bands around 398 and 334 cm^{-1} and are attributed to the $n \rightarrow \pi*$ and $\pi \rightarrow \pi*$ transitions, respectively.

μ_{eff} of Co(II) complexes were found to be 4.69–4.92 BM which assumed a octahedral geometry. The Ni(II) complexes showed μ_{eff} of 3.53–4.26 BM, which suggest an octahedral geometry. The Cu(II) complexes had μ_{eff} of 4.69–4.92 BM which assumed a octahedral geometry[26]. The magnetic moment of Zn(II)complexes where found to be in the range of (2.89-2.95 BM) which was consistent with the octahedral stereochemistry of the complexes.

Table 3: Electronic Spectral data of the Schiff base and its complexes

Mol. Formula	Abs. in nm	Transitions	Geometry
SB1 $C_{17}H_{14}N_2O_2S_2$	327	π-π*	-
$[Co(SB1)_2Cl_2]$ $C_{34}H_{28}N_4O_4S_4Cl_2Co$	436 433 737	$^4T_{1g}(F) \rightarrow {}^4T_{2g}(F)$ $^4T_{1g}(F) \rightarrow {}^4A_{2g}(F)$ $^4T_{1g}(F) \rightarrow {}^4T_{1g}(P)$	Oh.
$[Ni (SB1)_2Cl_2]$ $C_{34}H_{28}N_4O_4S_4Cl_2Ni$	422 439 763	$^3A_{2g}(F) \rightarrow {}^3T_{2g}(F)$ $^3A_{2g}(F) \rightarrow {}^3T_{1g}(F)$ $^3A_{2g}(F) \rightarrow {}^3T_{1g}(P)$	Oh.
$[Cu (SB1)_2Cl_2]$ $C_{34}H_{28}N_4O_4S_4Cl_2Cu$	742	$^2E_g \rightarrow {}^2T_{2g}$	Oh
$[Zn (SB1)_2Cl_2]$ $C_{34}H_{28}N_4O_4S_4Cl_2Zn$	398 334	$n \rightarrow \pi*$ $\pi \rightarrow \pi*$	Oh
SB2 $C_{21}H_{20}N_2O_4S$	330	π-π*	-
$[Co(SB2)_2Cl_2]$ $C_{42}H_{40}N_4O_8S_2Cl_2Co$	431 439 727	$^4T_{1g}(F) \rightarrow {}^4T_{2g}(F)$ $^4T_{1g}(F) \rightarrow {}^4A_{2g}(F)$ $^4T_{1g}(F) \rightarrow {}^4T_{1g}(P)$	Oh.
$[Ni(SB2)_2Cl_2]$ $C_{42}H_{40}N_4O_8S_2Cl_2Ni$	415 433 765	$^3A_{2g}(F) \rightarrow {}^3T_{2g}(F)$ $^3A_{2g}(F) \rightarrow {}^3T_{1g}(F)$ $^3A_{2g}(F) \rightarrow {}^3T_{1g}(P)$	Oh.
$[Cu(SB2)_2 Cl_2]$ $C_{42}H_{40}N_4O_8S_2Cl_2Cu$	740	$^2E_g \rightarrow {}^2T_{2g}$	Oh.
$[Zn(SB2)_2 Cl_2]$ $C_{42}H_{40}N_4O_8S_2Cl_2Zn$	396 332	$n \rightarrow \pi*$ $\pi \rightarrow \pi*$	Oh.

3.3. ^{1}H NMR and $^{[13]}$C NMR Spectra

The ^{1}H NMR spectra of Schiff base and the complexes were recorded in dmso-d_6. In the Schiff base ligand the peaks, in the range δ = 7.50–8.39 ppm were attributed to chemical shifts of the azomethine protons (HC=N) [27], and peak in the range δ = 5.32 ppm attributed to -NH_2 protons. In complexes the downfield shift of the azomethine proton and –NH_2 proton signals confirmed the formation of the metal complex[28]. Signals of aromatic and aliphatic protons were observed in the ranges 6.5–7.97 and 3.83 ppm, respectively.

Chemical shifts for ^{13}C NMR of ligands in DMSO-d_6 were recorded. The signals assigned to the chemical shifts of aromatic carbons were located at 113.6–152.2 ppm [29]. The signals observed at 152.8 and 160.2 ppm, were attributed to the chemical shifts of azomethine carbons which confirmed the formation of the Schiff bases.

3.4. Electrochemical Study

The cyclic voltammogram of $[Co(SB1)_2Cl_2]$ shows a well defined redox couple (Fig.1.a1) with reduction peak potential,(Epc) at -0.4V and 0.6V, the corresponding oxidation peak potential(Epa) at -0.6V and 0.15V. The peak separation of the redox couple was 0.2V and 0.45V. The ratio of the cathodic peak current, Ipc and anodic peak current, Ipa was found to be less than one which indicates that the electron transfer was quasireversible nature of the CoII/CoI redox couple. A cyclic voltammogram of Ni (II) complex [Ni $(SB1)_2Cl_2$] were presented in Fig.1.a2, voltammogram displays a reduction peak at Epc= 0.725V with an associated oxidation peak at Epa= -0.53V at a scan rate of 50mV/s. The peak separation of this couple (ΔEp) was 0.225V. The electrochemical behavior of [Cu $(SB1)_2Cl_2$] was shown in Fig. 1.a3, the CV displays two waves at Epc values -0.4 V and 0.8 V. When the potential scan in the positive direction was reversed at -0.625 V and 0.6 V. ΔEp value was (Epc - Epa) = 0.225V and 0.2V, the ratio *i*p,c /*i*p,a > 1 exhibited two quasi-reversible peaks. The Zn(II) complex exhibited two quasi-reversible peaks. A cyclic voltammogram of Zn(II) displays two reduction peaks at Epc= -0.575 V and 0.775V with an associated oxidation peaks at Epa= 0.325 V and 0.6V corresponding to the Zn(II)/Zn(I) at a scan rate of 50mV/s, it was evidence for quasi-reversible nature associated with one electron reduction [30].

The Co(II) complex $[Co(SB2)_2Cl_2]$ exhibits two electron quasi reversible transfer process with a reduction peak at Epc= -0.4V and 0.6V with a corresponding oxidation peak at Epa= -0.6V and 0.2 at a scan rate of 50mV/s (Fig.1.b1). The peak separation (ΔEp) of this couple was 0.2V and 0.4V. The difference between forward and backward peak potentials can provide a rough evaluation of the degree of the reversibility. The ratio of cathodic to anodic peak height was less than one. A cyclic voltammogram of Ni(II) complex [Ni $(SB2)_2Cl_2$] were presented in Fig. 2. Voltammogram displays a reduction peak at Epc= -0.4V and 0.575 with an associated oxidation peak at Epa= -0.625V and 0.15 V. The peak separation of this couple (ΔEp) was 0.225V and 0.425. This ΔEp value, evidence for the quasi-reversible Ni(II)/Ni(I) couple. The first reduction wave of the copper complexes [Cu $(SB2)_2Cl_2$] was safely assigned to the irreversible couple Cu(II)/Cu(I) with Epc = -0.70 and 0.775 Epa = -0.75V and 0.675V, ΔEp (Epc - Epa) = 0.05V and 0.150V. The ratio *i*p,c /*i*p,a > 1 confirms the irreversible nature of the electrode couple. The Zn(II) complex exhibited one quasi-reversible peak. A cyclic voltammogram

of Zn(II) displays one reduction peak at Epc= -0.175 V with an associated oxidation peak at Epa= 0.325 V corresponding to the Zn(II)/Zn(I) at a scan rate of 0.5 V/s, it was evidence for quasi-reversible nature associated with one electron reduction.

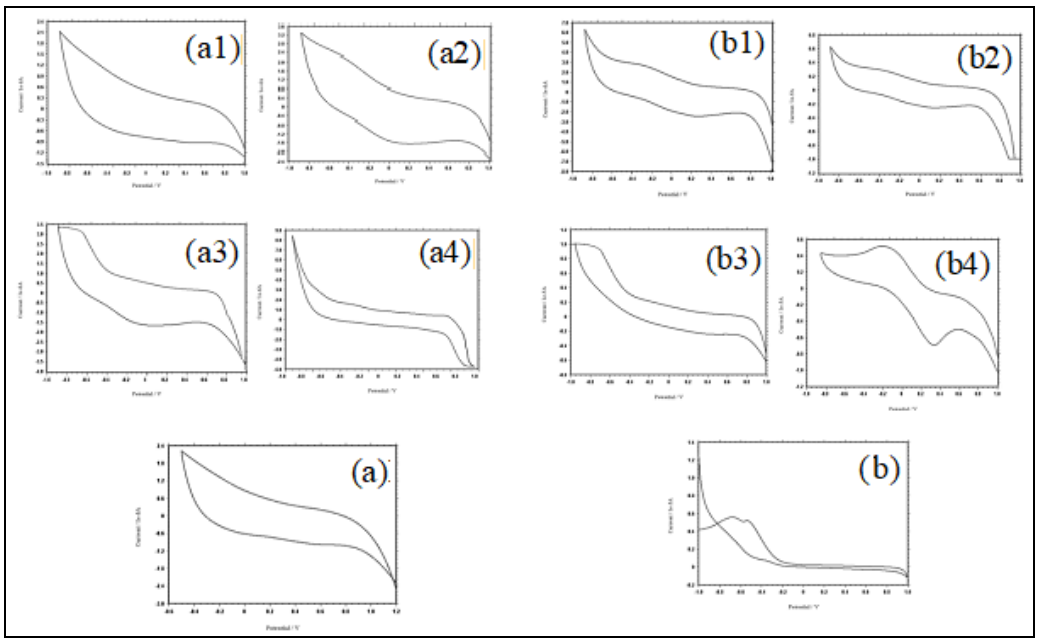

Fig 1: Cyclic voltammogram of (a)LigandSB1 (a1)[Co(SB2)$_2$Cl$_2$] (a2)[Ni(SB2)$_2$Cl$_2$] (a3)[Cu(SB2)$_2$Cl$_2$] (a4)[Zn(SB2)$_2$Cl$_2$] b)LigandSB2 (b1)[Co(SB2)$_2$Cl$_2$] (b2) [Ni(SB2)$_2$Cl$_2$] (b3) [Cu(SB2)$_2$Cl$_2$] (b4) [Zn(SB2)$_2$Cl$_2$]

Table 4: Cyclic Volametry data of the Schiff base and its complexes

Compound	Epc1	Epc2	Epa1	Epa2	Δ Ep1	Δ Ep2
[Co(SB1)$_2$Cl$_2$]	-0.4	0.6	-0.6	0.15	0.2	0.45
[Ni (SB1)$_2$Cl$_2$]	-0.35	-	-0.575	-	0.125	-
[Cu (SB1)$_2$Cl$_2$]	-0.4	0.8	-0.625	0.6	0.225	0.2
[Zn (SB1)$_2$Cl$_2$]	-0.575	0.775	-0.6	0.6	0.025	0.175
[Co(SB2)$_2$Cl$_2$]	-0.4	-0.6	0.6	0.2	0.2	0.4
[Ni (SB2)$_2$ Cl$_2$]	-0.4	-0.625	0.575	0.15	0.225	0.425
[Cu(SB2)$_2$ Cl$_2$]	-0.70	-0.75	0.775	0.675	0.05	0.150
[Zn (SB2)$_2$Cl$_2$]	-0.175	-	0.325	-	0.5	-

3.5. Corrosion studies

3.5.1. Chemical Method

The inhibition efficiency, corrosion rate and thermodynamic parameter values for mild steel in 1.0 M HCl media at different concentrations of the inhibitor were presented in Table 5.

Table 5. Inhibition efficiency, corrosion rate and free energy values at various concentrations of Schiff Base for the corrosion of mild steel in IM HCl obtained by weight loss measurements at 308 ±2K

Inhibitor	Inhi. Conc. (mM)	Weight Loss	N(mg/cm^{2}h)	Inhibition Efficiency ηw (%)	Degree of Coverage (θ)	-ΔG$_{ads}$ (kJ/mol)	ΔH$^o_{ads}$	ΔS$^o_{ads}$
Blank	-	0.0760	0.0633	-	-	-	-	-
SB1	0.2	0.0309	0.0258	59.31	0.5931	33.06	4460.03	14.59
	0.4	0.0283	0.0236	62.78	0.6278	31.66	4688.29	15.32
	0.6	0.0267	0.0223	64.83	0.6483	30.85	4833.39	15.79
	0.8	0.0256	0.0213	66.40	0.6640	30.29	4950.89	16.17
	1	0.023	0.0192	69.72	0.6972	30.11	5216.72	17.04
[Co(SB1)$_2$Cl$_2$]	0.2	0.0194	0.0162	74.45	0.7445	34.84	5651.84	18.46
	0.4	0.0177	0.0148	76.66	0.7666	33.37	5883.31	19.21
	0.6	0.0161	0.0134	78.86	0.7886	32.66	6137.81	20.03
	0.8	0.0162	0.0135	78.71	0.7871	31.90	6118.77	19.97
	1	0.0145	0.0121	80.91	0.8091	31.68	6399.16	20.88
[Ni(SB1)$_2$Cl$_2$]	0.2	0.0234	0.0195	69.24	0.6924	34.18	5177.01	16.92
	0.4	0.0219	0.0183	71.14	0.7114	32.63	5339.67	17.44

	0.6	0.0205	0.0171	73.03	0.7303	31.84	5513.37	18.00
	0.8	0.0175	0.0146	76.97	0.7697	31.64	5918.16	19.32
	1	0.0161	0.0134	78.86	0.7886	31.35	6137.81	20.03
$[Cu(SB1)_2Cl_2]$	0.2	0.0247	0.0206	67.51	0.6751	33.97	5036.47	16.46
	0.4	0.0226	0.0188	70.35	0.7035	32.54	5270.64	17.22
	0.6	0.0205	0.0171	73.03	0.7303	31.84	5513.37	18.00
	0.8	0.0195	0.0163	74.29	0.7429	31.27	5636.08	18.4
	1	0.0185	0.0154	75.71	0.7571	30.89	5781.54	18.87
$[Zn(SB1)_2Cl_2]$	0.2	0.0274	0.0228	64.04	0.6404	33.58	4776.61	15.62
	0.4	0.0253	0.0211	66.72	0.6672	32.11	4975.05	16.26
	0.6	0.0236	0.0197	68.93	0.6893	31.33	5150.88	16.83
	0.8	0.0218	0.0182	71.29	0.7129	30.88	5353.71	17.48
	1	0.018	0.015	76.34	0.7634	30.98	5848.94	19.09
SB2	0.2	0.0215	0.0179	71.77	0.7177	34.49	5396.27	17.63
	0.4	0.0213	0.0178	71.92	0.7192	32.73	5410.62	17.67
	0.6	0.0203	0.0169	73.34	0.7334	31.88	5543.5	18.10
	0.8	0.02	0.0167	73.66	0.7366	31.18	5573.99	18.20
	1	0.0198	0.0165	73.97	0.7397	30.65	5604.84	18.30
$[Co(SB2)_2\ Cl_2]$	0.2	0.0177	0.0148	76.66	0.7666	35.14	5883.31	19.22
	0.4	0.0164	0.0137	78.39	0.7839	33.62	6081.11	19.85
	0.6	0.014	0.0117	81.55	0.8155	33.09	6485.26	21.16
	0.8	0.0133	0.0111	82.49	0.8249	32.52	6620.08	21.60
	1	0.0126	0.0105	83.44	0.8344	32.12	6762.39	22.06
$[Ni(SB2)_2\ Cl_2]$	0.2	0.019	0.0158	75.08	0.7508	34.92	5715.87	18.67
	0.4	0.0171	0.0143	77.44	0.7744	33.48	5971.33	19.50
	0.6	0.0152	0.0127	79.97	0.7997	32.83	6275.22	20.48
	0.8	0.0141	0.0118	81.39	0.8139	32.33	6463.46	21.09
	1	0.0133	0.0111	82.49	0.8249	31.95	6620.08	21.60
$[Cu(SB2)_2\ Cl_2]$	0.2	0.0208	0.0173	72.71	0.7271	34.61	5483.59	17.92
	0.4	0.0195	0.0163	74.29	0.7429	33.04	5636.08	18.41
	0.6	0.0187	0.0156	75.39	0.7539	32.15	5748.49	18.77
	0.8	0.0177	0.0148	76.66	0.7666	31.59	5883.31	19.20
	1	0.0182	0.0152	76.03	0.7603	30.93	5815.02	18.98
$[Zn(SB2)_2\ Cl_2]$	0.2	0.0233	0.0194	69.40	0.6940	34.20	5190.18	16.96
	0.4	0.0207	0.0173	72.71	0.7271	32.83	5483.59	17.91
	0.6	0.0192	0.016	74.76	0.7476	32.07	5683.65	18.56
	0.8	0.0181	0.0151	76.18	0.7618	31.53	5831.92	19.04
	1	0.0154	0.0128	79.81	0.7981	31.5	6255.13	20.41

It can be seen from the data that the ligands and metal complexes showed appreciable corrosion inhibition behavior against corrosion of mild steel in a 1.0 M HCl solution. The metal complexes showed greater inhibition efficiency than free ligands. This may be attributed to the larger size of metal complexes. The value of corrosion rate decreased and inhibition efficiency increased with the inhibitor concentration. This trend may result from the fact that adsorption and surface coverage increased with the increase in ligands and metal complex concentrations. Thus, the order of efficiency of ligand SB1 and SB2 was $[Co(SB1)_2Cl_2]$ > $[Ni(SB1)_2Cl_2]$ > $[Zn(SB1)_2Cl_2]$ > $[Cu(SB1)_2Cl_2]$ > SB1 and $[Co(SB2)_2Cl_2]$ > $[Ni(SB2)_2Cl_2]$ > $[Zn(SB2)_2Cl_2]$ > $[Cu(SB2)_2Cl_2]$ > SB2 respectively. The difference inhibition efficiency might be due to the difference in the stability and solubility of complexes in the acid solution. The results show that the η_W (%) increases upon increasing the inhibitor concentration, this behavior explained strong interaction of the inhibitor molecule with the molecule with the metal surface resulting in adsorption.

3.5.2. Adsorption Isotherm and thermodynamic parameters

The adsorption isotherm can be determined if the inhibitor effect was due mainly to the adsorption on metallic surface (i.e. to its blocking). The adsorption isotherm type can provide additional information about the tested compounds properties. The fractional coverage surface (θ) can be easily determined from weight loss results shown in table 5.

The plots of Cθ versus C showed a linear correlation of slope close to unity suggesting that adsorption of thiosemicarbazide on mild steel interface obeys Langmuir adsorption isotherm.

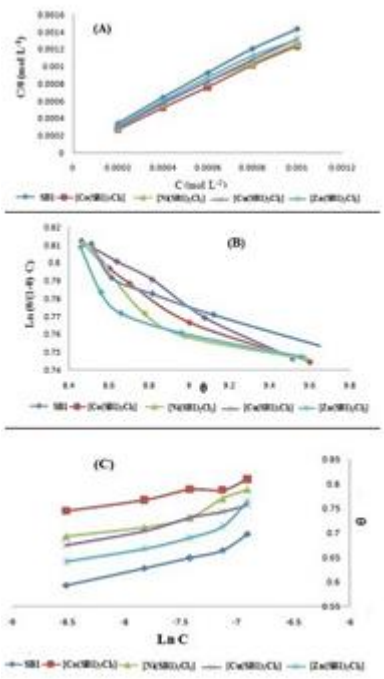

Fig.2.(A) Langmuir (B) Frumkin and (C) Temkin isotherm for the adsorption of ligand SB1 and its complexes

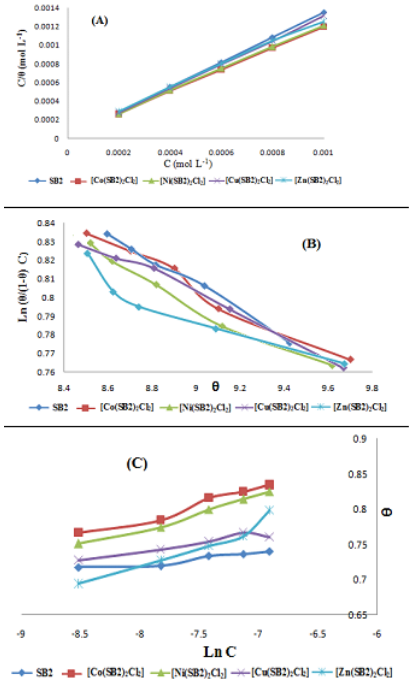

Fig.3.(A) Langmuir (B) Frumkin and (C) Temkin isotherm for the adsorption of ligand SB2 and its complexes

The values of heat of adsorption are less than - 40 KJ mol^{-1} suggesting the physical adsorption of the inhibitors [31]. The negative values of ΔG_{ads} suggest that the adsorption of thiosemicarbazide on mild steel is spontaneous. It is an established fact that values of ΔG_{ads} around -20 KJ mol^{-1} or less indicates physiosorption. The adsorption was attributed to the electrostatic attraction between the charged organic molecules and charged metal surface. The values of ΔG_{ads} around -40 KJ mol^{-1} or more are considered as chemisorptions. However, the values of ΔG_{ads} between -20 and -40 KJ mol^{-1} gives a disputed Judgment about the type of adsorption. In the present investigation the values of ΔG_{ads} were in the range of -30.06 to -36.26 KJ mol^{-1} suggesting a mixed type of adsorption involving both physiosorption and chemisoprtion.

3.5.3. Mechanism of inhibition

From the results obtained from weight loss and adsorption isotherm, it was concluded that Schiff Base ligands(SB1,SB2) and its metal complexes inhibits the corrosion of mild steel in 1.0 M HCl through its adsorption at the metal/solution interface. The adsorption of the inhibitor on the metal surface was a complexes phenomenon that can be considered as physio-chemisorption (mixed adsorption) rather than purely physical or chemical adsorption. The chemical adsorption occurs via donor-acceptor interactions between unshared electron pairs of heteroatom (such as N,O), π-electrons of the multiple bonds of aromatic rings and functional groups with the empty d-orbital of the surface iron atoms whereas the physical adsorption takes place via electrostatic interaction between the oppositely charged inhibitor molecule and metal surface. In the present study, the calculated ΔG_{ads} value were the range of -30.06 to -36.26 KJ mol^{-1} suggesting a mixed type of adsorption involving both physiosorption and chemisoprtion.

3.6. Antimicrobial Activity

Antibacterial and antifungal activity of Schiff base ligands and its cobalt, nickel and copper complexes were tested by well diffusion technique.

For *in vitro* antibacterial activity, the synthesized compounds were tested against the bacteria *Escherichia coli*, *Pseudomonas aeruginosa*, *Klebsiella pneumoniae*, *Proteus sps*, *Staphylococcus aureus*, *Enterococci sps and Starptococcus pyogenes* The present investigation suggest that all the metal complexes of the ligand bearing metal ion, -N =CH- group, have comparatively more biological activity. Antibacterial activity of metal chelates could be explained on the basis of chelation theory. On chelation, the polarity of the metal ion will be reduced to a greater extent due to the overlap of charge of the metal ion with donor groups. It was evident that overall potency of the ligands was enhanced on chelation. The antimicrobial activity significantly increased on coordination[32] with metal ions. Moreover, coordination reduces the polarity of the metal ion mainly because of the partial sharing of its positive charge with the donor groups[33] within the chelate ring system formed during coordination. From the antibacterial activity data, it was found that the antibacterial activity of $[Co(SB1)_2Cl_2]$ complex against *Escherichia coli* was higher activity than other complexes.

Similarly antifungal activity data (Table 7) indicated that the complexes had appreciable activity against *Aspergillus niger* and *Candida albicans* at one mg/ml concentration. Ligand has shown lesser activity as compared to the metal complexes.

Table 6: Antibacterial activities of Schiff base and its metal complexes

Compound	Antibacteria						
	E. coli	***P. aeruginosa***	***Klebsiella pneumoniae***	***Proteus sps***	***Staphylococcus aureus***	***Enterococci sps***	***Streptococcus pyogenes***
SB1	7.0	8.0	6.0	9.0	7.0	7.0	7.0
$[Co(SB1)_2Cl_2]$	20.0	11.0	15.0	11.0	13.0	16.0	18.0
$[Ni (SB1)_2Cl_2]$	12.0	10.0	9.0	12.0	10.0	17.0	9.0
$[Cu(SB1)_2Cl_2]$	10.0	12.0	17.0	12.0	9.0	12.0	17.0
$[Zn(SB1)_2Cl_2]$	10.0	13.0	16.0	10.0	9.0	15.0	9.0
SB2	9.0	10.0	8.0	7.0	11.0	9.0	6.0
$[Co(SB2)_2Cl_2]$	16.0	16.0	13.0	18.0	18.0	19.0	20.0
$[Ni(SB2)_2Cl_2]$	11.0	15.0	9.0	9.0	13.0	16.0	18.0
$[Cu(SB2)_2Cl_2]$	16.0	13.0	10.0	17.0	12.0	10.0	16.0
$[Zn(SB2)_2Cl_2]$	14.0	11.0	11.0	12.0	15.0	12.0	15.0
Chloramphe-nicol	22.0	21.0	20.0	22.0	23.0	20.3	23.0
Standard= 1mg/ml disc for bacteria							

Table 7: Antifungal activities of schiff base and its metal complexes

Compound	Antifungal		Compound	Antifungal	
	Aspergillus niger	***Candida albicans***		***Aspergillus niger***	***Candida albicans***
SB1	+	++	SB2	+	++
$[Co(SB1)_2Cl_2]$	++	+++	$[Co(SB2)_2Cl_2]$	++	+++
$[Ni (SB1)_2Cl_2]$	+++	++	$[Ni(SB2)_2Cl_2]$	+++	++
$[Cu (SB1)_2Cl_2]$	++	+++	$[Cu(SB2)_2Cl_2]$	++	+++
$[Zn (SB1)_2Cl_2]$	++	++	$[Zn(SB2)_2Cl_2]$	++	+++

Standard Nystatin= 100 units/disc for fungi.*Highly active = +++ (inhibition zone > 15mm);* Moderatively active = ++ (inhibition zone> 10mm)Slightly active = + (inhibition zone >5mm);

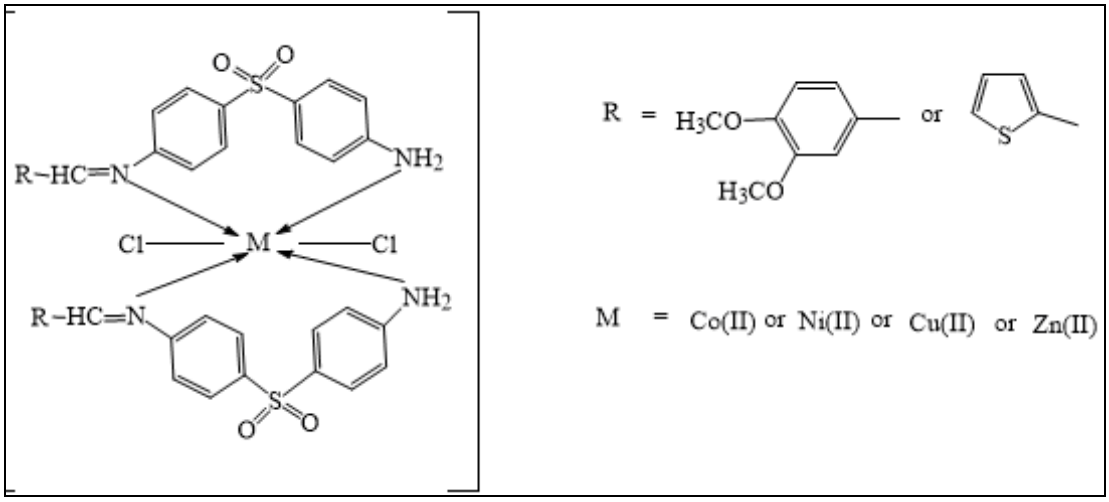

Fig 4: Structure of metal complexes

4. Conclusion

Co(II), Ni(II),Cu(II) and Zn(II) complexes of the Schiff base ligand derived from 4, 4- diaminodiphenylsulphone with 2-thiophenecarboxaldehyde and 3,4dimethoxybenzaldehyde were characterized using spectral and analytical data. The spectral data revealed that the Schiff base acts as a bidentate legend. The electrical and magnetic moment value of metal complexes has an octahedral geometry. The lower conductivity values of the complexes support the non-electrolytic nature of the metal complexes. On the basis of different techniques, the structure of the complexes was proposed (Fig.4). The electrochemical properties of the metal complexes revealed the quasi-reversible one electron/two electron transfer redox process. The ligands and metal complexes act as good corrosion inhibitors for mild steel in 1.0 M hydrochloric acid. The inhibition efficiency of the inhibitors increases with increase in concentration. The adsorptions of the inhibitors obey Langmuir, Frumkin and Temkin isotherms. The results showed that the $[Co(SB2)_2Cl_2]$ has excellent inhibition properties for the corrosion of mild steel in acid medium. The biological activity of the synthesized ligands and the metal complexes shows marked activity against the micro organisms.

5.Conflict of interest

The authors declare no conflict of interest.

6. References

1. Nabel NA, Zaki MF, Salem MAI. Colloids and Surface B, Biointerfaces. 2010; 77:96.
2. Lau KY, Mayr A, Cheung KK. Inor. Chem Acta. 1999; 285:223.
3. Vancoa J, Svajlenova O, Racanskac E, Muselika J. J Trace Elem. Med. Biol. 2004; 18:155.
4. Marcell DL, Thatyana RA, Erika MD, James LW, Marcus VN. Carbohydr. Res. 2009; 12:2042.
5. Mishra L, Singh VK. Indian J Chem. 1993; 37:446.
6. Raman N, Muthuraj V, Ravichandran S, Kulandaisamy AJ. Chem. Sci. 2003; 3:161.
7. Alhassan M, Chohan Z, Scozzafava A, Supuran C. J Enzyme Inhibition and Medicinal Chemistry. 2004; 19(3):263.
8. Mandell GL, Peri WA, Hardman JG, Limbid LE, Molinoff PB, Ruddon RW, *et al*. Pharmaceutical basis of therapeutics, 9th edition, McGraw_ Hill, New York, 1966, 1057.
9. Ajibola AO. Essential Medicinal Chemistry, 2nd Edn., Shaneson, New Jersey, 1999, 26.
10. Tella AC, Obaleye JA. E J Chem. 2009; 6:311.
11. Wolfgang K, Brigitte S. John Wiley & sons, England, 2006, 187.
12. Montgometry HE, Lingafelter C. J Phys. Chemi. 1960; 64:831.
13. Graziano JH, Siris ES, Lolacono NJ, Silverberg SJ, Turgeon L. Clin. Pharmcol. Ther. 1985; 37:431.
14. Patel AL, Chaudhary MJ. Inter. J Chem. Tech. Research. 2012; 4(3):918.
15. Aouniti A, Elmsellem H, Tighadouini S, Elazzouzi M, Radi S, Chetouani A, *et al*. J Taibah Uni. Sci., 2015: http://dx.doi.org/10.1016/j.jtusci. 2015.11.008
16. Hmamou DB, Salghi R, Zarrouk A, Messali M, Zarrok H, Errami M, *et al*. Der Pharma Chem. 2012; 4:1496.
17. Adejoro IA, Ojo FK, Obafemi SK. J Taibah Uni. Sci. 2015; 9:196.
18. Raman N, Ravichandran S, Thangaraja C. J Chemsci. 2004; 4:215.
19. Singh K, Barwa MS, Tyagi S. J Pharm. Res. 2007; 42:394.
20. Anitha C, Sheela CD, Tharmaraj P, Raja SJ. Spectrochimica Act. 2012; 98:35.
21. Patel AL, Chaudhary MJ. Inter. J Chem. tech Res. 2012; 3:918.
22. Karakucuk A, Iyido G, Demettas¸ Demir, Emine Elcin Oruc E, *et al*. Eur. J Med. 2011; 46:5616.
23. Manolov L, Raleva S, Genova P, Savov A, Froloshka L, Dundarova D. Bioinorg. Chem. Appl, 2006, 71938.
24. Chandra S, Kumar A. J Saudi Chem. Soc. 2007; 11:299.
25. Lever ABP. J Chem. Edu. 1968; 45:711.
26. Maruy RC, Patel P, Rajput S. Synthesis and reactivity in inorganic and metal-organic chemistry. 2003; 33(5):801.
27. Husain K, Bhat AR, Azam A. Eu. J Med. Chem. 2008; 43:2016.
28. Suni V, Kurup MRP, Nethaji M. Spectrochim Acta. 2006; 63:174.
29. Finkielsztein LM, Castro EF, Fabian LE, Moltrasio GY, Campos RH, Cavallaro LV, *et al*. Eur. J Med. Chem. 2008; 43:1767.
30. Bard AJ, Izatt LR. Electrochemical Methods: Fundamentals and Applications, 2nd ed., Wiley, New York, 2001.
31. Ebenso EE, Isabirye DA, Eddy NO. Int J Mol. Sci. 2010; 11:2473.
32. Shrinivasan D, Suresh T, Lakshmanaperumalsamly P. J Ethanopharmacol. 2001; 74:220.
33. Sengupta SK, Pandey OP, Srivastava BK, Sharma VK. Trans. Met. Chem. 1998; 23(4):349.